

# Bloch oscillations in complex crystals with $\mathcal{PT}$ symmetry

S. Longhi

*Dipartimento di Fisica and Istituto di Fotonica e Nanotecnologie del CNR,  
Politecnico di Milano, Piazza L. da Vinci 32, I-20133 Milano, Italy*

Bloch oscillations (BO) in complex lattices with  $\mathcal{PT}$  symmetry are theoretically investigated with specific reference to optical BO in photonic lattices with gain/loss regions. Novel dynamical phenomena with no counterpart in ordinary lattices, such as non-reciprocal BO related to violation of the Friedel's law of Bragg scattering in complex potentials, are highlighted.

PACS numbers: 42.50.Xa, 42.70.Qs, 11.30.Er, 72.10.Bg

Bloch oscillations (BO), i.e. the coherent oscillatory motion of a quantum particle in a periodic potential driven by an external dc force, represent one of the most striking predictions of wave mechanics of periodic systems. In the quantum realm, BO have been experimentally observed for electrons in semiconductor superlattices [1] and for ultracold atoms or Bose-Einstein condensates in tilted optical lattices [2]. Classical analogues of BO have been also proposed and observed for optical [3] and acoustical [4] waves. The phenomenon of BO is related to the transition of energy spectrum from continuous (energy bands) to (nearly) discrete, with the formation of Wannier Stark (WS) ladders when the dc force is applied. In physical space, BO are generally explained in terms of wave Bragg scattering off the periodic potential, causing a wave packet to oscillate rather than translate through the lattice. Previous studies on BO have considered particle motion in real-valued potentials, may be in presence of nonlinearity, lattice disorder or particle interactions [5]. However, particle or wave dynamics in complex potentials is not uncommon in physics [6–9]. Complex potentials for matter waves emerge in the near resonant interaction of light with open two-level systems [7], whereas in optics wave propagation in lossy or active waveguides is described by a complex refractive index [8]. Complex potentials have received in recent years an enormous interest since the discovery that non-Hermitian Hamiltonians with parity-time ( $\mathcal{PT}$ ) symmetry may possess an entirely real-valued energy spectrum below a phase transition (symmetry-breaking) point [10].  $\mathcal{PT}$  Hamiltonians belong to the more general class of pseudo-Hermitian systems [11]. Optical realizations of  $\mathcal{PT}$ -symmetric potentials, based on light propagation in coupled waveguides with a complex refractive index, have been recently proposed [12–14], whereas energy band formation and spontaneous symmetry-breaking thresholds have been investigated in a few  $\mathcal{PT}$  potential models [15] and in presence of nonlinearity [16] or lattice disorder [17]. It is the aim of this Letter to investigate the onset of BO in periodic lattices with  $\mathcal{PT}$  symmetry, highlighting some unique features arising from the complex nature of the scattering potential. We consider here BO for light waves in photonic lattices [3], however the analysis can be applied to other physical systems, such as to matter waves in accelerating complex optical lattices.

Paraxial propagation of light at wavelength  $\lambda$  in a weakly-guiding one-dimensional waveguide lattice with a superimposed transverse refractive index gradient is described by the Schrödinger-type equation [13, 18]

$$i\lambda\partial_z\psi = -\frac{\lambda^2}{2n_s}\partial_x^2\psi + V(x)\psi + Fx\psi \equiv (\mathcal{H}_0 + Fx)\psi \quad (1)$$

where  $\lambda = \lambda/(2\pi)$  is the reduced wavelength,  $n_s$  is the substrate refractive index,  $V(x) = n_s - n(x)$  is the potential,  $n(x) = n(x+a)$  is the refractive index profile of the lattice (spatial period  $a$ ), and  $F$  is the refractive index gradient which mimics an external dc force. For  $F = 0$ ,  $\mathcal{PT}$  symmetry requires  $V(-x) = V^*(x)$ , i.e. suitable combinations of optical gain and loss regions in the lattice, as discussed in [12–14]. The real and imaginary parts of the potential are denoted by  $V_R(x)$  and  $\alpha V_I(x)$ , respectively, where  $\alpha \geq 0$  is a dimensionless parameter that measures the anti-Hermitian strength of  $\mathcal{H}_0$ . For given profiles of  $V_R$  and  $V_I$ , the spectrum of  $\mathcal{H}_0$  turns out to be real-valued and composed by bands separated by gaps for  $\alpha < \alpha_c$ , where  $\alpha_c \geq 0$  corresponds to the spontaneous symmetry breaking point. For  $\alpha \geq \alpha_c$ , band merging and appearance of pairs of complex-conjugates eigenvalues is observed [13, 15]. For instance, for the potential

$$V_R(x) = V_0 \cos(2\pi x/a), \quad V_I(x) = V_0 \sin(2\pi x/a) \quad (2)$$

one has  $\alpha_c = 1$  [13].

Let us first consider the case  $\alpha < \alpha_c$ , and indicate by  $\phi_n(x, \kappa) = u_n(x, \kappa) \exp(i\kappa x)$  the Bloch-Floquet eigenfunction of  $\mathcal{H}_0$ , corresponding to the  $n$ -th lattice band and to wave number  $\kappa$  in the first Brillouin zone ( $-\pi/a \leq \kappa < \pi/a$ ) with periodic part  $u_n(x, \kappa)$ . Thus  $\mathcal{H}_0\phi_n(x, \kappa) = E_n(\kappa)\phi_n(x, \kappa)$ , where  $E_n(\kappa)$  is the real-valued band dispersion curve. As for real potentials, one can show that  $E_n(-\kappa) = E_n(\kappa)$ . Additionally,  $\text{Re}(u_n(\kappa, x))$  and  $\text{Im}(u_n(\kappa, x))$  have well defined and opposite parity under the inversion  $x \rightarrow -x$ , whereas  $\phi_n^\dagger(x, \kappa) = \phi_n(-x, -\kappa)$  are eigenfunctions of the adjoint  $\mathcal{H}_0^\dagger$  with same eigenvalues  $E_n(\kappa)$ . Assuming that  $I_n \equiv \int_0^a dx u_n^*(-x, -\kappa)u_n(x, \kappa)$  does not vanish, i.e. in absence of spectral singularities, the orthonormal conditions  $\langle \phi_l^\dagger(x, \kappa') | \phi_n(x, \kappa) \rangle \equiv \int_{-\infty}^{\infty} dx \phi_l^{\dagger*}(x, \kappa')\phi_n(x, \kappa) = D_n \delta_{n,l} \delta(\kappa - \kappa')$  hold, where  $D_n = \pm 1$  is given by the

sign of  $I_n$  in each band [10, 13]. To investigate WS localization, like in ordinary crystals we expand the wave packet  $\psi$  as a superposition of Bloch-Floquet states [19],  $\psi(x, z) = \sum_n \int d\kappa c_n(\kappa, z) \phi_n(\kappa, z)$ . The scalar product of both sides of Eq.(1) with  $\langle \phi_n^\dagger(x, \kappa) |$  yields the following evolution equations for the spectral coefficients  $c_n(\kappa, z)$

$$i\lambda \left( \partial_z - \frac{F}{\lambda} \partial_\kappa \right) c_n = E_n(\kappa) c_n + F \mathcal{D}_n \sum_l X_{n,l}(\kappa) c_l \quad (3)$$

where  $X_{n,l}(\kappa) \equiv (2\pi i/a) \int_0^a dx u_n^*(-x, -\kappa) \partial_\kappa u_l(x, \kappa)$ . The off-diagonal elements  $X_{n,l}$  ( $n \neq l$ ) in Eq.(3) are responsible for interband transitions, i.e. Zener tunneling (ZT), and can be written in the equivalent form  $X_{n,l} = (2\pi\lambda^2/an_s)[E_n(\kappa) - E_l(\kappa)]^{-2} \int_0^a u_n^*(-x, -\kappa) \partial_x V(x) u_l(x, \kappa)$ . If bands  $n$  and  $l$  are separate by a large gap and the force  $F$  is small enough such that  $F|X_{n,l}(\kappa)| \ll |E_n(\kappa) - E_l(\kappa)|$  in the entire Brillouin zone, ZT is negligible as in ordinary lattices [19]. Taking  $X_{n,l} \simeq 0$  for  $n \neq l$  (single-band approximation), the WS spectrum of the  $n$ -th band is then obtained by letting in Eq.(3)  $c_n(\kappa, z) = a_n(\kappa) \exp(-iEz/\lambda)$  and imposing the boundary condition  $a_n(2\pi/a) = a_n(0)$ . This yields

$$E_l^{(n)} = Fla + \langle E_n \rangle + i\gamma_n \quad (l = 0, \pm 1, \pm 2, \dots), \quad (4)$$

where we have set  $\langle E_n \rangle = (a/2\pi) \int_{-\pi/a}^{\pi/a} d\kappa E_n(\kappa)$  and  $\gamma_n = (D_n Fa/2\pi) \int_{-\pi/a}^{\pi/a} d\kappa \text{Im}(X_{n,n}(\kappa))$ . As compared to an ordinary crystal [19], the main difference here is that the WS ladder spectrum is complex-valued, even though  $\alpha < \alpha_c$ . This is simply due to the fact that the external force  $F$  breaks the  $\mathcal{PT}$  symmetry of the Hamiltonian. In each ladder, the imaginary parts of the eigenvalues have the same value (i.e., independent of  $l$ ), equal to  $\gamma_n$ . Since  $\text{Im}(X_{n,n}(\kappa))$  is an even function of  $\kappa$ ,  $\gamma_n$  is usually non-vanishing, and its sign is reversed as the direction of the force, i.e. the sign of  $F$ , changes. Therefore, in complex lattices below the phase transition point, BO with spatial period  $z_B = \lambda/(Fa)$  are observed, however they are either amplified or damped depending on the sign of  $F$ . This behavior is illustrated in Fig.1, which shows the onset of amplified or damped BO as obtained by numerical simulations of Eq.(1) for the complex lattice of Eq.(2) with  $\alpha = 0.3$  and for an input excitation of the lattice with a broad Gaussian beam at normal incidence. In the figures, the evolution of the total beam power  $P = P(z)$  is also shown. Note that, in spite all WS eigenvalues have the same imaginary part,  $P(z)$  shows a non-exponential behavior, with abrupt changes of  $P(z)$  in correspondence of Bragg scattering of the beam from the lattice. This behavior is ascribable to the non-orthogonality of WS states in complex potentials.

As the non-Hermitian parameter  $\alpha$  is increased to cross the phase transition value  $\alpha_c$ , gap narrowing till band merging, associated to the appearance of pairs of complex-conjugate eigenvalues, is observed [13], making

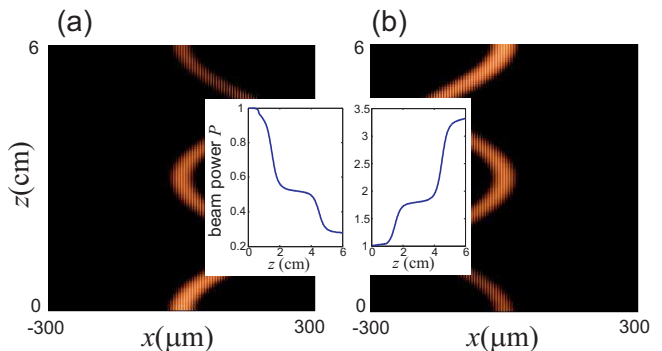


FIG. 1: (color online) BO in the complex lattice of Eq.(2) for  $\alpha = 0.3$  and for an index gradient (a)  $F = -3.52 \text{ m}^{-1}$ , and (b)  $F = 3.52 \text{ m}^{-1}$ . Other parameter values are  $a = 6 \text{ }\mu\text{m}$ ,  $\lambda = 633 \text{ nm}$ ,  $V_0 = 0.001$ , and  $n_s = 1.42$ . The figures show the evolution of field amplitude  $|\psi(x, z)|$  and beam power  $P = \int dx |\psi(x, z)|^2$  (normalized to the input power) versus propagation distance  $z$ . The BO period is  $z_B = 3 \text{ cm}$ .

the previous analysis inapplicable. Here we will limit to investigate the onset of BO in the  $\alpha = \alpha_c$  and  $\alpha > \alpha_c$  regimes by considering two specific examples which enable an analytical treatment.

The first example is given by the potential (2) at

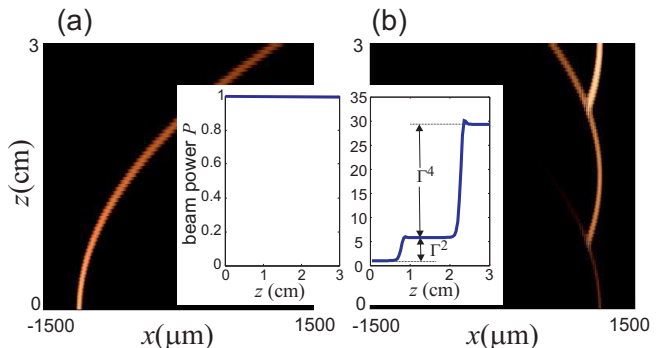


FIG. 2: (color online) Same as Fig.1, but for  $\alpha = \alpha_c = 1$  and (a)  $F = -7.03 \text{ m}^{-1}$ , (b)  $F = 7.03 \text{ m}^{-1}$ . Other parameter values are as in Fig.1, except for  $V_0 = 2 \times 10^{-4}$ . Note that BO disappear for a negative index gradient  $F$ .

the phase transition point  $\alpha = \alpha_c = 1$ , i.e.  $V(x) = V_0 \exp(2\pi i x/a)$  [20], for which band gaps disappear and the energy dispersion is described by the free-particle parabola  $E(\kappa) = (\lambda^2/2n_s)\kappa^2$ , periodically folded inside the first Brillouin zone. In presence of an external force  $F$ , numerical simulations indicate that the wave packet evolution strongly depends on the sign of  $F$ , as shown in Fig.2. Remarkably, BO disappear for  $F < 0$ , and the wave packet propagates following a parabolic path as if the complex lattice were absent [Fig.2(a)]. This result indicates that a net drift along the lattice can be achieved by the application of a dc force, an effect which is not possible in ordinary crystals without collisions. Conversely, for  $F > 0$  an oscillatory dynamics survives, with spatial period equal to  $z_B = \lambda/(Fa)$  [Fig.2(b)]. In this case,

at propagation distances corresponding to Bragg reflection from the lattice, a rather abrupt amplification of the scattered beam is observed [see the inset of Fig.2(b)]. This dynamical regime, which can be referred to as unidirectional BO, has no counterpart in ordinary lattices and is related to violation of Friedel's law of Bragg scattering by complex potentials [7, 20], i.e. breakdown of Bragg diffraction invariance by crystal inversion. Analytical insights into unidirectional BO can be gained by writing Eq.(1) in momentum space and assuming that the lattice is excited by a broad wave packet at normal incidence, i.e.  $\psi(x, 0) = \int dk g(k) \exp(-ikx)$ , where the plane-wave spectrum  $g(k)$  is narrow at around  $k = 0$  with a spectral width much smaller than the Bragg wave number  $k_B = 2\pi/a$ . Let us indicate by  $\psi_0(x, z)$  the propagated wave packet that one would observe in absence of the lattice, i.e. the solution to Eq.(1) with  $V = 0$ . The center of mass  $\langle x \rangle(z)$  of  $\psi_0(x, z)$  follows the parabolic path  $\langle x \rangle(z) = -(F/2n_s)z^2$  due to the external force  $F$ , whereas the mean value of momentum  $\langle k \rangle$  grows linearly,  $\langle k \rangle(z) = -Fz$ . In presence of the complex lattice, Bragg diffraction sets in when  $\langle \kappa \rangle$  gets close to  $-k_B/2$ , but not when  $\langle \kappa \rangle \sim k_B/2$ ; this nonreciprocal behavior of Bragg scattering by complex potentials is discussed e.g. in [7, 20]. In presence of the lattice, one can show that the wave packet is expressed by a superposition of retarded wave packets  $\psi_0(x, z - nz_B)$  with amplitudes  $B_n(z)$ , namely

$$\psi(x, z) \simeq \sum_{n=0}^{+\infty} B_n(z) \psi_0(x, z - nz_B). \quad (5)$$

In Eq.(5),  $B_0(z) = 1$ , whereas for  $n \geq 1$  the amplitudes  $B_n$  can be iteratively calculated from the relation

$$B_n(z) = -i \frac{V_0}{\lambda} \int_0^z d\xi \exp[-i\varphi_n(\xi)] B_{n-1}(\xi), \quad (6)$$

where we have set  $\varphi_n(z) = (\lambda^2 k_B / 2n_s F) [(Fz/\lambda - k_B n)^2 + k_B (Fz/\lambda - k_B n) + k_B^2 / 3]$ . In the limit  $z_B \gg (n_s a / \pi F)^{1/2}$  and for  $F < 0$ ,  $|B_{n \geq 1}(z)|$  remains small because of  $\varphi_n(z)$  has no stationary points for  $z > 0$ . Physically, this corresponds to the absence of Bragg scattering (the condition  $\langle k \rangle \sim -k_B/2$  is never satisfied), and the scenario of Fig.2(a) is observed. Conversely, for  $F > 0$  the phase  $\varphi_n$  has a stationary point at  $z = z_B(n - 1/2)$ , and one obtains  $|B_n(z)| \sim \Gamma^n H(z - nz_B + z_B/2)$ , where  $\Gamma \equiv (V_0/\lambda)(n_s a/F)^{1/2}$  and  $H(\xi)$  is the Heaviside step function [ $H(\xi) = 0$  for  $\xi < 0$ ,  $H(\xi) = 1$  for  $\xi > 0$ ]. In this case, Eq.(5) clearly shows that a periodic regeneration and amplification of the wave packet  $\psi_0$  due to Bragg scattering occurs at  $z = z_B/2, 3z_B/2, 5z_B/2, \dots$ , explaining the behavior observed in Fig.2(b). For parameter values used in the simulations, the predicted value of amplification factor  $\Gamma$  is  $\Gamma \simeq 2.186$ , with which the staircase behavior of beam power shown in the inset of Fig.3(b) is reproduced with excellent accuracy.

As a second example, we consider a complex binary lattice [16] with broken  $\mathcal{PT}$  symmetry at  $\alpha_c = 0$ , and

show that the external force can restore a real-valued energy spectrum. The lattice consists of an array of equally-spaced single-mode waveguides with alternating gain ( $V_I > 0$ ) and loss ( $V_I < 0$ ) channels, i.e.  $V_R(x) = \sum_l h(x - la - a/2)$  and  $V_I(x) = \sum_l (-1)^l h(x - la - a/2)$ , where  $h(x) = h(-x)$  defines the (real) index profile of the waveguide channel (see Fig.3(a)). Note that, for  $\alpha \neq 0$ , the lattice period is  $2a$ . A typical band diagram is shown in Fig.3(b). In the tight-binding approximation and for  $\alpha \ll 1$ , light transport in the lattice is described by coupled-mode equations for the modal amplitudes  $a_l$  of light trapped in the waveguides [3, 16, 18, 21]

$$i \frac{da_l}{dz} = -\frac{\Delta}{4} (a_{l+1} + a_l) + f l a_l + i(-1)^l \frac{g}{2} a_l \quad (7)$$

where  $\Delta/4$  is the real-valued coupling rate between ad-

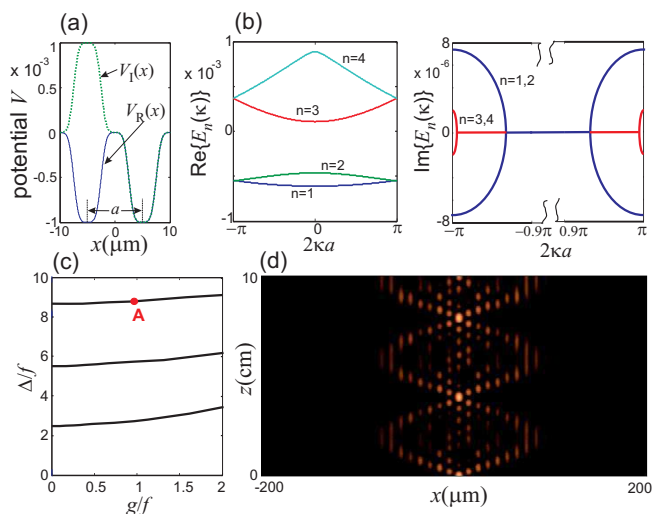


FIG. 3: (color online) BO in a complex binary lattice ( $a = 10 \mu\text{m}$ ). (a) Profiles of  $V_R$  and  $V_I$ , and (b) corresponding band diagram for  $\alpha = 0.01$  (real and imaginary parts of energy  $E$ ). (c) Resonance curves in the  $(\Delta/f, g/f)$  plane corresponding to a real-valued WS ladder spectrum. (d) Breathing BO mode (single waveguide input excitation) for  $F = 1.618 \text{ m}^{-1}$ , corresponding to a Bloch period  $z_B \simeq 39.1 \text{ mm}$ .

acent waveguides,  $f = Fa/\lambda$ , and  $g$  is the real-valued power gain/loss coefficient in the waveguides, which is proportional to  $\alpha$ . For the potential of Fig.3(a) with  $\alpha = 0.01$ , from the band diagram of Fig.3(b) (the two merged bands  $n = 1$  and  $n = 2$ ) one can estimate  $g \simeq 1.46 \text{ cm}^{-1}$  and  $\Delta \simeq 14 \text{ cm}^{-1}$ . For  $F = 0$ , the spectrum of Eq.(7) is purely continuous and composed by two merged minibands [the two lowest bands of Fig.3(b)], namely [16]

$$E(\kappa) = \pm \lambda \sqrt{(\Delta/2)^2 \cos^2(\kappa a) - (g/2)^2}, \quad |\kappa| \leq \pi/2a. \quad (8)$$

Since complex-conjugate eigenvalues appear near the band edges for any value of  $g > 0$ , the lattice has zero threshold for  $\mathcal{PT}$  symmetry-breaking, i.e.  $\alpha_c = 0$ . In presence of the external force  $F$ , the spectrum becomes

purely discrete and composed by two interleaved WS ladders  $E_l^{(1)}$  and  $E_l^{(2)}$ , as in a binary lattice with real potential [21]. Specifically, one can show that

$$E_l^{(1,2)} = 2Fal - \frac{Fa\varphi_{1,2}}{\pi} + i\frac{Fa \ln|y_{1,2}|}{\pi} \quad (9)$$

( $l = 0, \pm 1, \pm 2, \dots$ ) where  $y_{1,2} \equiv |y_{1,2}| \exp(i\varphi_{1,2}) = \text{Re}(\sigma) \pm [1 + \text{Re}(\sigma)^2]^{1/2}$ ,  $\sigma \equiv \mathcal{S}_{1,2}$ , and the  $2 \times 2$  matrix  $\mathcal{S}$  is the propagator for the differential system  $dx_{1,2}/d\kappa = \pm i(\Delta/4f) \cos(\kappa/2)x_{1,2} + (g/4f)x_{2,1}$  from  $\kappa = 0$  to  $\kappa = 2\pi$ . Note that the two WS ladders are generally complex-valued with opposite sign of their imaginary part. However, if the condition  $\text{Re}(\sigma) = 0$  is satisfied,  $y_{1,2} = \pm 1$  and the spectrum becomes real-valued and given by a single WS ladder, namely  $E_l = Fal$  ( $l = 0, \pm 1, \pm 2, \dots$ ). Figure 3(c) depicts the numerically-computed locus in the  $(\Delta/f, g/f)$  plane where  $\text{Re}(\sigma) = 0$ , showing the existence of a sequence of resonance curves. A perturbative calculation of the propagator  $\mathcal{S}$  in the  $g \rightarrow 0$  limit shows that the resonance curves depart from the points of the  $\Delta/f$  axis that are the roots of Bessel function  $J_0$  [21]. Along such resonance curves, a forced Bloch particle undergoes undamped nor amplified BO, with spatial period  $z_B = \lambda/(Fa)$ . This is shown in Fig.3(d), which depicts an example of a BO breathing mode, obtained by numerical analysis of Eq.(1) for single waveguide excitation of the complex binary lattice of Fig.3(a), with a forcing

$F = 1.618 \text{ m}^{-1}$ , corresponding to point A ( $g/f \simeq 0.91$ ,  $\Delta/f \simeq 8.72$ ) on the third resonance curve of Fig.3(c). Photonic  $\mathcal{PT}$  lattices may provide an accessible laboratory to experimentally observe BO in complex crystals. Complex refractive indices could be realized in engineered arrays of active semiconductor waveguides with selective pumping to achieve gain and loss regions. At optical or near-infrared wavelengths, a modulation depth of the imaginary refractive index  $\Delta n_I \sim 2 \times 10^{-4}$  (as in Fig.2) requires a gain/absorption coefficient of the order  $\sim 10\text{-}20 \text{ cm}^{-1}$ , which is available with current semiconductor optical amplifier technology. Smaller gain/loss coefficients are needed for the example of Fig.3. Non-reciprocal BO could be also observed in passive (i.e. without gain) waveguide arrays with loss modulation, in a geometrical setting similar to the one recently realized to demonstrate  $\mathcal{PT}$  symmetry breaking in a passive AlGaAs optical coupler [22]. The transverse index gradient can be realized by either chirping the waveguide width [3] or by waveguide axis bending [18]. In conclusion, BO in complex crystals with  $\mathcal{PT}$  symmetry behave differently than in ordinary lattices owing to non-reciprocity of Bragg scattering. Our results indicate that the conventional wisdom of BO and transport for classical or matter waves needs to be modified when dealing with complex crystals.

- 
- [1] C. Waschke, H. G. Roskos, R. Schwedler, K. Leo, H. Kurz, and K. Köhler, *Phys. Rev. Lett.* **70**, 3319 (1993).  
[2] M. BenDahan, E. Peik, J. Reichel, Y. Castin, and C. Salomon, *Phys. Rev. Lett.* **76**, 4508 (1996); S. R. Wilkinson, C. F. Bharucha, K. W. Madison, Q. Niu, and M. G. Raizen, *Phys. Rev. Lett.* **76**, 4512 (1996); B.P. Anderson and M. A. Kasevich, *Science* **282**, 1686 (1998).  
[3] R. Morandotti, U. Peschel, J. S. Aitchison, H. S. Eisenberg, and Y. Silberberg, *Phys. Rev. Lett.* **83**, 4756 (1999); T. Pertsch, P. Dannberg, W. Elfle, A. Bräuer, and F. Lederer, *Phys. Rev. Lett.* **83**, 4752 (1999); H. Trompeter, T. Pertsch, F. Lederer, D. Michaelis, U. Streppe, A. Bräuer, and U. Peschel, *Phys. Rev. Lett.* **96**, 023901 (2006).  
[4] H. Sanchis-Alepuz, Y.A. Kosevich, and J. Sanchez-Dehesa, *Phys. Rev. Lett.* **98**, 134301 (2007).  
[5] D. Cai, A.R. Bishop, N. Grønbech-Jensen, and M. Salerno, *Phys. Rev. Lett.* **74**, 1186 (1995); F. Dominguez-Adame, V.A. Malyshev, F.A.B.F. de Moura, and M.L. Lyra, *Phys. Rev. Lett.* **91**, 197402 (2003); A. Buchleitner and A.R. Kolovsky, *Phys. Rev. Lett.* **91**, 253002 (2003).  
[6] N. Hatano and D.R. Nelson, *Phys. Rev. Lett.* **77**, 570 (1996).  
[7] C. Keller, M.K. Oberthaler, R. Abfalterer, S. Bernet, J. Schmiedmayer, and A. Zeilinger, *Phys. Rev. Lett.* **79**, 3327 (1997).  
[8] A. Kostenbauder, Y. Sun, and A.E. Siegman, *J. Opt. Soc. Am. A* **14**, 1780 (1997).  
[9] M.V. Berry, *Czech. J. Phys.* **54**, 1039 (2004).  
[10] C.M. Bender and S. Boettcher, *Phys. Rev. Lett.* **80**, 5243 (1998); C.M. Bender, *Rep. Prog. Phys.* **70**, 947 (2007).  
[11] A. Mostafazadeh, *J. Math. Phys.* **43**, 2814 (2002).  
[12] R. El-Ganainy, K. G. Makris, D. N. Christodoulides, and Z. H. Musslimani, *Opt. Lett.* **32**, 2632 (2007).  
[13] K.G. Makris, R. El-Ganainy, D.N. Christodoulides, and Z.H. Musslimani, *Phys. Rev. Lett.* **100**, 103904 (2008).  
[14] S. Klaiman, U. Günther, and N. Moiseyev, *Phys. Rev. Lett.* **101**, 080402 (2008).  
[15] C.M. Bender, G.V. Dunne, P.N. Meisinger, *Phys. Lett. A* **252**, 272 (1999); H.F. Jones, *Phys. Lett. A* **262**, 242 (1999); Z. Ahmed, *Phys. Lett. A* **286**, 231 (2001); A. Khare and U. Sukhatme, *J. Math. Phys.* **47**, 062103 (2006); T. Curtright and L. Mezincescu, *J. Math. Phys.* **48**, 092106 (2007).  
[16] Z.H. Musslimani, K.G. Makris, R.El-Ganainy, and D.N. Christodoulides, *J. Phys. A* **41**, 244019 (2008).  
[17] O. Bendix, R. Fleischmann, T. Kottos, and B. Shapiro, *Phys. Rev. Lett.* **103**, 030402 (2009).  
[18] S. Longhi, *Laser & Photon. Rev.* **3**, 243 (2009).  
[19] J. Callaway, *Quantum Theory of the Solid State* (Academic Press, New York, 1974), pp. 465-478; V. Grecchi and A. Sacchetti, arXiv:quant-ph/0506057.  
[20] M.V. Berry, *J. Phys. A* **31**, 3493 (1998).  
[21] B.M. Breid, D.Witthaut, and H.J. Korsch, *New J. Phys.* **8**, 110 (2006); F. Dreisow, A. Szameit, M. Heinrich, T. Pertsch, S. Nolte, A. Tünnermann, and S. Longhi, *Phys. Rev. Lett.* **102**, 076802 (2009).  
[22] A. Guo, G.J. Salamo, D. Duchesne, R. Morandotti, M.

Volatier-Ravat, V. Aimez, G. A. Siviloglou, and D. N. Christodoulides, Phys. Rev. Lett. **103**, 093902 (2009).